

Clustering for power system stability using graph theory and electrical distance

Illia Diahovchenko ^{a,b,*}, Andrew Keane ^a

^a School of Electrical and Electronic Engineering, University College Dublin, Dublin, Ireland

^b Electric Power Engineering Department, Sumy State University, Sumy, Ukraine



ARTICLE INFO

Keywords:

Clustering
Critical energy infrastructure
Graph theory
Electrical distance
Stability
Synchronous generator
Dynamic simulations

ABSTRACT

Modern power systems are increasingly threatened by disruptions, including terrorist and military attacks targeting critical energy infrastructure. Disruptions to electric power plants and bulk substations can result in wide-area blackouts, significant economic damage, and endanger public safety. Therefore, efficient preparation and prompt operational responses to threats are essential for power systems' stability and resiliency. This study introduces a novel approach for cluster formation within transmission power systems using graph theory metrics and electrical distance. Clusters enable selective dynamic and steady-state simulations, focusing on vulnerable areas and optimizing computational resources and time. The proposed clustering approach offers scalability and can enhance operational preparedness against potential disruptions and abrupt changes in generation after attacks on critical energy infrastructure or unexpected outages, which makes it useful for transmission system operators. It can also assist with the planned integration of renewable energy sources into bulk power systems, enabling more efficient analysis of their impacts on system stability and performance.

1. Introduction

1.1. Problem statement

While cyberattacks on critical energy infrastructure have become a recognized threat that can lead to cascading failures in power systems [1] and attracted wide attention from researchers and policymakers, there are limited reports of physical attacks targeting power plants and bulk substations. The work [2] provides examples of terrorist attacks by the Islamic State on the energy sector in Iraq and Syria, which included the capture of power plants and damage to refineries and gas processing stations. Attacks on electricity-generating plants, transmission lines, water pumping stations, oil refineries, and environmental facilities in Syria, Libya, and Yemen are documented in the article [3].

Since Russia's full-scale invasion of Ukraine in 2022, the Ukrainian energy system has become a "legitimate military target", with attacks intensifying since the spring of 2024 [4]. Multiple examples of strikes on electrical infrastructure with long-range cruise missiles, ballistic missiles, combat drones, and loitering munitions have been reported, escalating the resiliency threats for energy systems to an unprecedented level [4–9].

Between March and May 2024, Ukraine lost 9 GW of generation capacity, predominantly from thermal and hydroelectric power-generating units, which significantly impaired the country's energy infrastructure and left it with about one-third of its pre-war generation capacity [5]. By June 2024, 73 % of the thermal power plants and 20 hydroelectric generation units were rendered inoperative due to extensive destruction [6]. Additionally, 18 large combined heat and power plants, 800 boiler houses, about 50 % of extra high voltage, and many distribution substations were damaged or completely destroyed, causing intermittent outages and emergency blackouts in different parts of the national power system despite ongoing repairs [5,7].

The Ukrainian power plant's private operator DTEK has reported that its stations lost 80 % of their capacity in the attacks [8]. After the destruction of the Trypillskaya thermal power plant during a massive attack in April 2024, the state-owned PJSC Centrenenergo lost 100 % of its generation capacities [9]. By May 2024, the losses incurred by the national power companies were estimated at over \$18 billion [6].

While localized terrorist or military attacks can render particular power plants or substations inoperable, a coordinated strike on multiple generation sites could disrupt synchronization across the entire

* Corresponding author at: School of Electrical and Electronic Engineering, University College Dublin, Dublin, Ireland.
Email address: illia.diahovchenko@ucd.ie (I. Diahovchenko).

grid, severely affect operations, cause substantial economic losses, and compromise public safety. With Ukraine being a part of the Continental Europe Synchronous Area, as shown in Fig. 1, the related operational disruptions may spread beyond the national grid [10]. In practical terms, a major disruption in Ukraine's power system could have cross-border impacts, such as frequency deviations or overloading in connected systems, potentially causing cascading failures or requiring corrective load shedding.

At the same time, the share of renewable energy sources (RESs) in power systems keeps growing at an accelerating pace, and in 2023 their share of total power generation reached 30 % [12]. As more variable energy resources, like wind and solar power plants, are integrated into the power system, the variability and uncertainty in electricity generation increase [13]. The fluctuations in RES output can result in frequency instability or voltage control issues, particularly when the capacity for flexible generation or storage is limited.

Given the increased risks of attacks on critical energy infrastructure and the challenges brought by the growing share of RESs, proper preparation for operational disruptions is essential for system stability satisfaction. This preparation would start with studying the post-contingency operation of the national and interconnected power systems in both steady state and dynamics, followed by the development of anticipation strategies, such as preventive reconfiguration, load shedding, and consolidating the efforts for rapid repairs of facilities for a faster recovery [14].

A static solution shows the state of the power system at a particular point in time, and this type of simulation is usually fast and readily processed by commercial-grade software. On the other hand, dynamic simulations of large electrical networks present challenges related to their complexity and the number of dynamic parameters involved. Dynamic studies can require a high computational resources and time to run. In addition, some disturbances have only local impacts, requiring a detailed dynamic representation at the local level [15].

A bulk power system can be divided into clusters to overcome the named limitations. This would enable the selective performance of detailed post-contingency static and dynamic simulations selectively, only for the influenced areas.

1.2. How can the clustering problem be amended?

The effectiveness of selective studies relies on the appropriate partitioning of the bulk power system and the selection of relevant clusters for further simulation and analysis. Determining the boundaries of clusters can be based on the concept of electrical distance, which is defined as the measure of the impedance or electrical path length between two buses in the power system [16]. This concept has been used to address several power-systems-related problems [16–27].

The authors of Ref. [17] examined the structure of the French extra high voltage network, aiming to divide it into uncoupled zones and choosing a descriptive node (a pilot node) for each zone, which would support secondary voltage control and coordination of different generating sets at a regional level. They determined the voltage drops between the pilot node and the other nodes and identified the pilot node, which “seems to be the closest electrically for each node of the system” [17]. The paper [18] introduces a method of transmission charge of power contracts allocation based on the relative electrical distance concept. The work [19] describes methods for dividing a power network into zones, such that buses are electrically close to other buses within zones. The definition of zones using electrical distance rather than asset ownership or historical affiliation has the potential to improve the utility of planning procedures, such as load deliverability assessment, that are based on zone boundaries [19]. Particularly, this approach aims to guarantee that a localized area has adequate capacity resources to maintain reliability during a local capacity emergency while ensuring that the transmission network facilitates energy exchange between these areas. Further, the article [20] demonstrates solving a multi-attribute partitioning problem of power networks based on electrical distance, seeking to minimize distances between nodes within a zone and maximize distances between nodes in different zones. Here, the zones within a power system are understood as collections of buses such that buses within a zone are strongly connected, and buses between zones are weakly connected [20]. The paper [16] introduces a method to divide bulk power systems into clusters, considering them as electrical-distance-based graphs and applying graph theory analysis. The authors of Ref. [21] employed a contingency analysis tool and considered the electrical proximity of buses to identify the most vulnerable transmission connections.

The study [22] compares impedance-based, sensitivity-based, and transient-based electrical distance methods for clustering power systems, emphasizing their suitability for various applications, such as voltage control and dynamic stability. The simulation results show that the examined methods adequately capture electrical coupling between nodes, although with varying performance levels [22]. In the work [23], electrical similarity, derived from voltage fluctuations, is used as a clustering metric to partition power systems into loosely coupled zones for voltage control and islanding strategies. A clustering algorithm based on Mixed Integer Linear Programming formulation, considering the network's layout, the electrical losses along lines, and the reliability aspects is presented in [28]. The authors of Ref. [24] proposed a stability-focused controlled islanding scheme using the density-based clustering algorithm and the system electrical distance from wide-area measuring system data.

Purely topological power system models offer limited insight into how a system will behave, as they neglect the physical flow equations that govern power propagation through the network. In the work [25], it is demonstrated that layouts based on power transfer distance provide greater visual separation between nodes, reducing congestion and creating a design that is both visually appealing and meaningful. The authors of Ref. [26] argue that the topological comparisons of electrical networks with graphs do not account for the physical laws of the power flows, namely Ohm's and Kirchhoff's laws. As an alternative, they represent the electrical structure as a weighted graph, which is based on the electrical distance rather than on the topological connections. The paper [27] introduces the effective graph resistance metric to relate the topology of a power grid to its robustness against cascading failures while

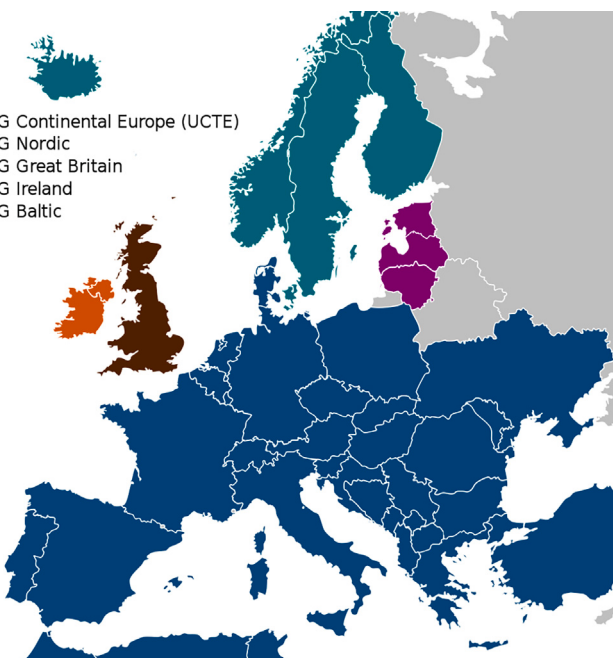


Fig. 1. Continental Europe synchronous area [11].

also considering the fundamental characteristics of the electric power grid, such as power flow allocation according to Kirchhoff's laws. By clustering electricity and gas infrastructures based on graph theory metrics, the study [29] identifies critical nodes and subnetworks, supporting enhanced planning for random and targeted disruptions.

Although the contribution of the previous research is significant, novel solutions are needed to further enhance the preparedness of bulk power systems against physical attacks targeting critical energy infrastructure components and to avoid potential disruptions due to variability in electricity generation by RESs. With this aim, a graph theory-supported approach has been developed to identify clusters within large national and interconnected power networks, using their electrical distance matrices as a representation. By identifying clusters of interest and simulating in detail only those clusters instead of the entire system, the time for simulations and analysis can be minimized, lowering the requirements for high-performance computing resources. As a result, quicker responses to contingency events and operational decisions will be fostered.

The proposed solution builds upon the method outlined in [16]. However, this work substantially extends the findings presented in [16] by enhancing the literature survey, expanding the methodology and explaining it in more detail, providing additional experimental results, comparing the proposed approach with a commonly used technique, and further analysis of the findings.

Compared to the solutions from the related studies, the proposed approach combines the advantages of both graph theory and electrical distance, resulting in better scalability. Particularly, it can be useful due to the following aspects:

- graph theory allows considering the entire topology and relationships between buses and enhances adaptability;
- the concept of electrical distance does not depend on specific fault scenarios and can be applied under varying operating conditions;
- graph theory metrics and electrical distance can be computationally efficient for large systems, especially when implemented using algorithms like Floyd–Warshall or Dijkstra's [30].

By employing the proposed approach, transmission system operators (TSOs) can improve the effectiveness and reduce the time of the simulations focused on voltage stability, transient stability, frequency stability, RES integration, resiliency and system restoration. As a result, TSOs will be enabled to analyze faster the effects of disruptions caused by the loss of power plants or bulk substations in specific areas. They can also assess transmission constraints and evaluate how RESs with unstable output impact certain regions of the power system. On the other hand, grid planners can prioritize the development, refinement, and updating of models for the most critical zones within a bulk power system.

2. Methodology

2.1. Obtaining a matrix of electrical distances

In this paper, the power system is treated as an undirected graph $G = (N, E)$, where generators and transmission buses are the set of nodes $N = [n, \dots, N]$, and the connections between them are the set of edges $E \in N \times N$. It is also assumed that the graph contains no self-loops: $(i, i) \notin E$ for all $i \in N$.

Following up on the earlier point, electric power obeys Kirchhoff's laws and flows through all available paths rather than following a distinct path (e.g., the shortest path). Therefore, the notion of distance in power grids needs to be tailored based on power systems' fundamentals. One of the simplest measures of electrical distance for a power system is the absolute value of the inverse of its admittance matrix [19]:

$$\text{EID}_{\text{raw}} = |\mathbf{Y}_{\text{syst}}^{-1}| \quad (1)$$

For instance, the matrix $\mathbf{Y}_{\text{syst}} = [y_{vu}]$ defines the admittance between the connected buses v and u , which is the weight of the edge

$(v, u) \in E$. In electrical power systems theory, the admittance matrix is equivalent to the weighted Laplacian matrix of a power grid, which reflects the interconnection of buses with transmission lines [27] and, therefore, captures the topological structure of an electrical network. In this case, the weights of the links between the nodes v and u correspond to the complex admittance value y_{vu} , comprised of conductance g_{vu} and susceptance b_{vu} parts, between the respective nodes. When multiple interconnecting lines exist between the buses, the connection is set to one edge $(v, u) \in E$ by recalculating the admittance.

The bus admittance matrix can be defined as [21]:

$$\mathbf{Y}_{\text{syst}} = \begin{cases} g_{vu} + jb_{vu} & \text{if } v \neq u \\ -\sum(g_{vu} + jb_{vu}) & \text{if } v = u \\ 0 & \text{if no connection exist} \end{cases} \quad (2)$$

By definition, the \mathbf{Y}_{syst} tends to be sparse as the value of some entries is 0 if nodes v and u do not have a direct physical connection.

The matrix obtained from (1) is nothing but the impedance matrix. To get a better representation of the electrical distance matrix, this study takes some alternative steps.

First, the impedance matrix is obtained as the inverse of the system admittance matrix:

$$\mathbf{Z}_{\text{syst}} = -1j \cdot (\mathbf{Y}_{\text{syst}}^{-1}) \quad (3)$$

After the inversion, the inverse of the admittance matrix is multiplied by $-1j$ to obtain the impedance matrix. The reason for this step can be explained as follows. The impedance is a complex-valued quantity that includes both resistance (a real-valued quantity) and reactance (an imaginary-valued quantity). The inverse of the admittance matrix represents the inverse of the conductances (g_{vu}) and susceptances (b_{vu}) of the elements (i.e., links between the v -th and u -th buses) in the system. To obtain the impedance matrix, one needs to take the reciprocal of these values and multiply by $-1j$ to convert the conductances to resistances r_{vu} and the susceptances to reactances x_{vu} .

The authors of Ref. [25] simply used the off-diagonal elements of a system's \mathbf{Z}_{syst} matrix to populate a system distance matrix. The diagonal elements of the \mathbf{Z}_{syst} matrix are not generally zero, suggesting that it does not inherently encode distance information.

For the present work, the requirement for zeros on the main diagonal is artificially enforced to populate the complex electrical distance matrix as follows.

$$\text{EID}_{\text{cplx}} = \begin{cases} z_{vu} = r_{vu} + jx_{vu} & \text{if } v \neq u \\ 0 & \text{if } v = u \end{cases} \quad (4)$$

The equivalent electrical distance between nodes v and u is, thus, given by the magnitude of the relevant entry of the \mathbf{Z}_{syst} . A small value of z_{vu} corresponds to a shorter electrical distance (as the impedance-weighted value) but denotes a stronger coupling between v and u . This reflects a more significant propensity for power exchange between these nodes. For example, parallel transmission lines can strengthen the line as the power flowing through it gets divided according to Kirchhoff's law, given that loading does not change. In this case, the electrical distance of the line will be reduced [21].

For transmission lines with a high ratio of reactance to resistance (X/R ratio), the behavior of transmission branches can be represented through reactance only, especially for steady-state analysis. If the impedance matrix is calculated from b_{vu} values only (i.e., the admittance matrix contains only susceptances to simplify the calculation), the multiplication by $-1j$ in (3) will not compromise the results, since the electrical distance is calculated from absolute values of an impedance matrix:

$$\text{EID} = |\mathbf{Z}_{\text{syst}}| \quad (5)$$

Thus, the electrical distance matrix EID gives an idea about the sensitivity between voltage and current changes for every pair of nodes. To

summarize, the matrix with electrical distances of a power system can be obtained from an impedance matrix of a power system, which, in turn, can be obtained from an admittance matrix of the same system. While this topological approach is conceptually plain, it requires inverting a sparse matrix of the rank equal to the number of network nodes.

In the simplest variant, the Z_{syst} can be obtained with the direct inversion methods, which work well for small power systems (possibly up to several hundred buses). However, more computationally efficient methods may be required for large sparse matrices. For the purposes of this study, five matrix inversion methods were used in Python to obtain the impedance matrix:

1. the direct NumPy inversion function;
2. the LU decomposition;
3. the SciPy solver for the sparse linear systems;
4. the QR decomposition;
5. the blockwise matrix inversion [31].

The user should select the most suitable technique based on the specific characteristics of the system being analyzed. For smaller electrical networks, the direct NumPy inversion works well, while for large networks, more advanced matrix decomposition methods should be preferred.

2.2. Metrics selection

To understand how well a power system can maintain its stability and functional integrity during disruptions, it is necessary to evaluate its operational efficiency and robustness [29]. Several graph theory metrics were selected to assess the connectivity, efficiency, and overall structure of the electrical-distance-based system's graph G represented with the matrix **EID**.

- **Diameter.** The diameter is the longest shortest path length between any two vertices in the graph. It represents the maximum electrical distance between any pair of vertices:

$$D = \max(d(v, u)), \forall(v, u), \quad (6)$$

where $d(v, u)$ represents the electrical distance (shortest path length) between vertices v and u .

- **Average path length (APL).** It is the average of the shortest path lengths between all pairs of vertices in the graph. This metric provides a measure of the typical electrical distance between vertices in the graph.

$$APL = \frac{1}{N(N - 1)} \cdot \sum d(v, u), \forall(v, u), \quad (7)$$

where N is the total number of vertices (i.e., buses) in a power system; $d(v, u)$ represents the electrical distance (shortest path length) between the vertices v and u .

- **Eccentricity.** The eccentricity of a vertex v is the maximum electrical distance between that vertex and any other vertex in the graph. The minimum eccentricity among all vertices gives insight into the overall size of the graph.

$$E(v) = \max(d(v, u)), \forall u \quad (8)$$

- **Radius.** The radius of a graph is the minimum eccentricity among all vertices. It represents the smallest maximum electrical distance from any vertex to all other vertices.

$$R = \min(E(v)), \forall v \quad (9)$$

- **Effective Graph Resistance (EGR).** Computation of the EGR for a power grid can be done by aggregating the effective resistances between each pair of nodes [27]:

$$EGR = \sum_{v=1}^N \sum_{u=v+1}^N ER(v, u), \quad (10)$$

where $ER(v, u)$ is the effective resistance between vertices v and u . The effective resistance $ER(v, u)$ is the potential difference between the nodes v and u when a unit current is injected at node v and withdrawn at node u . Thus, the EGR is the sum of the individual effective resistances between each pair of nodes in the network.

The EGR can be used to relate a power system's topology to its robustness against cascading failures. An increase in EGR reduces the robustness of a power system [27].

- **Efficiency.** This is a measure of how effectively information can be transmitted across the graph. It is calculated as the reciprocal of the average path length. This metric can provide information about the overall reachability of the vertices.

$$Eff = \frac{1}{APL} \quad (11)$$

It should be noted that the selected metrics assume the electrical distances are accurately represented in the graph, and they may vary depending on the specific algorithm or definition used to calculate the electrical distances. Moreover, the connectivity of the power system's graph should be considered separately from the sparsity or density of the inverted matrix. The density or sparsity of the inverted matrix is influenced by the specific properties of the power system, such as the network's connectivity, the arrangement of lines and buses, and the physical layout. However, it is not a direct indicator of the connectivity of a power system's graph.

The connectivity of a power system's graph is determined by the presence of paths between buses, regardless of the sparsity or density of the matrix representation. Therefore, a power system can have a sparse matrix representation and still be fully connected if there are paths between all buses, even if the inverted matrix is not dense. For instance, the sparsity of the inverted matrix Z_{syst} depends on the sparsity pattern of the original matrix Y_{syst} representing the admittances of the lines between buses.

If the original Y_{syst} matrix has a sparse structure with many zero elements representing non-connected buses or lines, the inverted Z_{syst} matrix may retain sparsity to some extent. However, the sparsity pattern does not provide direct information about the connectivity of the power system.

2.3. Defining a cluster within a bulk system

By estimating the calculated metrics, the user establishes the electrical-distance-based threshold beyond which the electrical connection between an i -th bus and the cluster-forming bus (i.e., the starting bus) is considered "weak" so that the i -th bus is not included in the cluster. Defining this threshold is not always straightforward and requires understanding the essence of graph theory and knowledge of the particular power system. To assist the user with setting the clustering threshold, an initial approximation for determining the threshold can be used, which is according to the equation [16]:

$$\xi_{\text{threshold}} = \max(\xi_1, \xi_2), \quad (12)$$

where the thresholding options ξ_1 and ξ_2 are calculated as

$$\xi_1 = D - \frac{D - \min(R, APL)}{2} \quad (13)$$

$$\xi_2 = \frac{EGR}{N(N - 1)} \quad (14)$$

Additional attention should be paid to the efficiency values: higher Eff indicates well-integrated power systems with smaller reliance on long-distance transmission.

Clustering is performed using [Algorithm 1](#).

Algorithm 1 Electrical-distance-centered clustering with graph theory.

```

Require: EID           ▷ CSC-type matrix of electrical distances
Require:  $\xi_{\text{threshold}}$     ▷ User-defined distance threshold
Require:  $\beta_{\text{bus}}$         ▷ Initial bus for clustering
Ensure:  $B_{\text{cluster}}$       ▷ Set of buses in the cluster
1: Initialize  $B_{\text{cluster}} \leftarrow \{\}$                                 ▷ Empty cluster
2: Add  $\beta_{\text{bus}}$  to  $B_{\text{cluster}}$ 
3: for each branch connected to  $\beta_{\text{bus}}$  do
4:   Extract TO BUS and weight from EID
5:   if weight <  $\xi_{\text{threshold}}$  then
6:     Add TO BUS to  $B_{\text{cluster}}$ 
7:   Traverse branches connected to TO BUS recursively
8:   end if
9: end for
return  $B_{\text{cluster}}$ 

```

The cluster, B_{cluster} , is expanded by appending TO BUS numbers of all the branches through which the algorithm has travelled if the weights of those branches are below the user-defined threshold.

Two algorithms for finding shortest paths in a weighted graph have been implemented and tested for clustering [32] – Floyd–Warshall and Dijkstra's:

- Floyd–Warshall algorithm can find shortest paths in a directed weighted graph with positive or negative edge weights; a single execution of the algorithm will find the lengths of the shortest paths between all pairs of vertices;
- Dijkstra's algorithm finds the shortest path between a given node (the “source node”) and all other nodes in a graph. This algorithm uses the weights of the edges to find the path that minimizes the total distance (weight) between the source node and all other nodes.

The developed approach was implemented in Python scripts and is independent of the power system simulation software.

2.4. Assessing practicability of the created clusters

The formation of clusters aims to ensure computational efficiency while accurately capturing the system's dynamic behavior. The buses near the fault or disturbance location are most likely to be influenced and, therefore, are expected to be included in the clusters. Also, the algorithm should select the buses where load or generation is highly sensitive to the disturbances.

To justify the practicability of the proposed clustering approach, it should be compared to relevant existing techniques. One such technique is based on voltage sensitivity across the power system [22]. The degree of voltage coupling between the node pairs can be measured by the attenuation of voltage variations between them [17,22]. This method is directly related to Kirchhoff's Current and Voltage laws: when a fault occurs, the fault current flows through paths determined by the network's impedances. Therefore, buses with lower impedance in the fault current's path are more directly affected by the disturbance and, as a result, experience larger voltage drops.

Therefore, the bus voltage sag after a disturbance can be used to identify buses that might be prone to voltage instability, if their voltage values after the fault clearance are below the thresholds specified in the grid codes. The condition for sorting out those buses can be expressed with the equation:

$$V_{\text{fault},i} \leq V_{\text{lim}}^{\max}, \quad (15)$$

where $V_{\text{fault},i}$ is the post-disturbance voltage value at the i -th bus; V_{lim}^{\max} is the voltage threshold, below which the bus is considered as affected by the disturbance.

The critical clearing time (CrCT) and the cluster's size are selected as the main criteria for comparison. The CrCT is the maximum time for

which a disturbance can persist without causing the power system to lose stability and can be expressed by the formula:

$$\text{CrCT} = \max\{t_{\text{stbl}}\}, \quad (16)$$

where t_{stbl} is the largest fault duration for which the system remains stable.

The system's stability assessment checks whether the rotor angle of a synchronous machine exceeds a threshold value and is performed according to the binary search algorithm from Ref. [33].

The simulations are iterative and are based on the system dynamics, so the CrCT is subject to stability checks at each step [33]. First, an initial fault duration time (i.e., a small initial guess) and the maximum fault duration (i.e., a considerable time beyond which instability is guaranteed) are selected. Then, a three-phase short circuit fault is applied over a candidate time, $t_{\text{cand},n}$. If the system remains stable for the fault duration, the next candidate time is doubled, and the CrCT calculation attempt is repeated. If the system becomes unstable, the candidate time is reduced to the midpoint between the last stable and current unstable durations:

$$t_{\text{cand},n+1} = \frac{t_{\text{stbl}} + t_{\text{unstbl}}}{2}, \quad (17)$$

where t_{unstbl} is the fault duration beyond which the system becomes unstable.

The stopping condition for this algorithm is

$$|t_{\text{unstbl}} - t_{\text{stbl}}| \leq \Delta t, \quad (18)$$

where Δt is the time step of the simulation.

2.5. Power system reduction using the clustering results

When simulating the dynamic behavior of a subset of the power system (i.e., a cluster), it is necessary to eliminate unnecessary details to accelerate the simulations and reduce computational complexity. This can be done in several ways:

1. By creating an equivalent representation of the portion of the bulk system that is not explicitly modeled. The dynamic equivalencing includes the separation of the cluster from the external system and replacing the latter with an equivalent that behaves similarly but has fewer components. Techniques for impedance reduction and aggregation of generators are used to reduce the external system.
2. By removing the generator dynamic models and keeping only the governor and/or exciter models for electrical machines not included in the cluster.
3. By replacing full generator models with simpler equivalents for electrical machines not included in the cluster, which allows for retaining some level of dynamic behavior.

Each of these ways has its pros and cons. Techniques for impedance reduction and generator aggregation, such as Ward or radial equivalent independent (REI) [34], are commonly used to reduce the external system's size through a process that iteratively removes nodes from the network. However, it is challenging to identify boundary buses that separate the cluster from the external system: since clusters are formed based on electrical distance rather than topological proximity, the selected buses may be spread across the network rather than concentrated in one area.

Deactivation of the dynamic models of some generators and running the simulation with only a subset of generators having dynamic models can be valid for studying the dynamics of a specific area in a bulk power system. However, the system's overall dynamic response will be affected because the neglected generators do not provide system inertia or participate in transient stability and frequency regulation. This increases the risk of unrealistic results because of interactions between

the dynamically and statically modeled generators. Keeping only the governors' dynamic models for the external part of the power system allows frequency response but no voltage dynamics, while keeping only the exciters' dynamic models allows voltage regulation but no frequency response. Yet, additional differential equations still need to be solved, which requires computational power.

The third approach – replacing complex generator models in the external system with simpler equivalent models – allows for reducing the simulation complexity while maintaining some level of dynamic behavior. This strategy is selected for this study as the most suitable for the proposed electrical-distance-centered clustering method.

3. Results and discussion

The “savnw” test case available in the PSS/E software package and the standard IEEE 39-bus system were selected for the case study demonstrations.

3.1. SAVNW test case

3.1.1. Cluster formation

The “savnw” system has 23 buses, 6 generators, and 8 loads distributed between three areas; the nominal frequency is 60 Hz. Its single-line diagram is shown in Fig. 2. For dynamic simulations in PSS/E, the “savnw” test case incorporates GENROU and GENSAL synchronous generator models for salient-pole machines, IEEET1 and SEXS excitation system models, and TGOV1 and HYGOV turbine-governor models [33].

Table 1

Results of electrical-distance-centered cluster formation using graph theory for the “savnw” test case.

Starting bus	Clustered buses
101	101, 3001, 3002, 3003, 3004, 3005, 3011
102	102, 3001, 3002, 3003, 3004, 3005, 3011
154	154, 3001, 3002, 3003, 3004, 3005, 3011
206	206, 3001, 3002, 3003, 3004, 3005, 3011
211	211, 3001, 3002, 3003, 3011
3011	101, 102, 151, 152, 153, 154, 201, 202, 203, 204, 205, 206, 211, 3001, 3002, 3003, 3004, 3005, 3006, 3007, 3008, 3011, 3018
3018	3001, 3002, 3003, 3004, 3005, 3006, 3007, 3008, 3011, 3018

The main inputs for the electrical-distance-centered clustering using graph theory are a starting bus number, which would be a bus of a targeted generation plant, and an algorithm for building up a cluster, as explained in Section 2.

By selecting the buses of power plants or bulk substations at risk and setting the value of $\xi_{\text{threshold}}$, the cluster(s) within a large power system can be created accordingly. The results of the cluster margins' determination with the proposed method for the “savnw” test system are summarized in Table 1. The cluster-forming threshold, $\xi_{\text{threshold}}$, was set to 0.06 for all the considered generation buses. Clustering with both Floyd–Warshall and Dijkstra's algorithms gave similar results, confirming the correctness of the implementation.

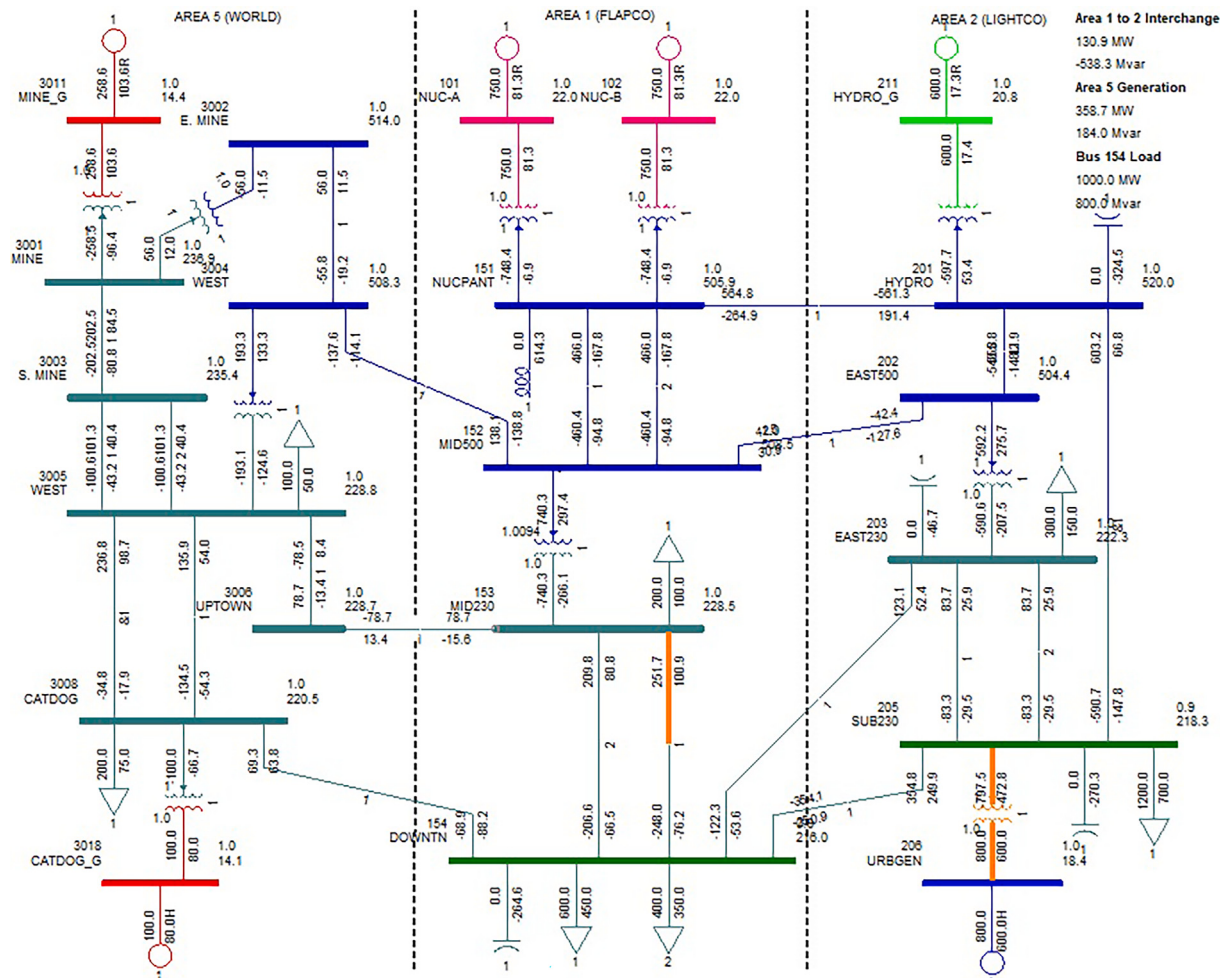


Fig. 2. Single-line diagram of the industrial workshop power system.

Table 2

Results of cluster formation for the “savnw” test case, based on the post-disturbance voltage sag.

Starting bus	Clustered buses
101	101, 102, 151, 152, 153, 154, 201, 202, 203, 204, 205, 3004, 3005, 3006, 3007, 3008
102	101, 102, 151, 152, 153, 154, 201, 202, 203, 204, 205, 3004, 3005, 3006, 3007, 3008
154	151, 152, 153, 154, 201, 202, 203, 204, 205, 206, 3001, 3002, 3003, 3004, 3005, 3006, 3007, 3008, 3011, 3018
206	152, 153, 154, 201, 202, 203, 205, 206, 3004, 3005, 3006, 3007, 3008, 3018
211	151, 152, 153, 154, 201, 202, 203, 204, 205, 211, 3006, 3007, 3008
3011	153, 154, 3001, 3002, 3003, 3004, 3005, 3006, 3007, 3008, 3011, 3018
3018	3008, 3018

It should be noted that the clustered buses are not necessarily neighboring vertices of the graph G . From Table 1, it can be seen that, e.g., the cluster formed around the nuclear power plant at Bus 101 includes 7 buses, around the hydro power plant at Bus 31 – only 5 buses, and at Bus 3011 – all the 23 buses of the “savnw” test case example. On average, a cluster contains 9.43 buses.

The buses numbered 3001, 3002, 3003, and 3011 are present in all cluster-forming scenarios from Table 1, which indicates their sensitivity to possible contingencies and highlights the vulnerability of the “World” area (Area 5) of the “savnw” test case.

Next, the clusters for the “savnw” test case were defined based on the voltage sag after a disturbance. Three-phase short circuit faults were applied at the same starting buses as per Table 1. The voltage threshold for this power system is assumed to be $V_{\text{lim}}^{\max} = 0.7 \text{ p.u.}$ All the buses where the voltage sags below this limit are considered to be severely affected by the disturbance and will be sorted into a cluster. The simulation results are summarized in Table 2.

From Table 2, it can be seen that the cluster formed around the nuclear power plant at Bus 101 has 16 buses, around the hydro power plant at Bus 31 – 13 buses, and at Bus 3011 – 11 buses of the “savnw” test case. In general, the clusters formed on the criterion of the post-disturbance voltage sag are notably bigger compared to the clusters formed according to the electrical-distance-centered approach with graph theory applied. An average cluster from Table 2 contains 13.29 buses.

The buses numbered 3004, 3005, 3007, and 3008 are present in most clusters formed based on post-disturbance voltage sag. These buses also belong to the “World” area (Area 5) of the “savnw” test case example, indicating their sensitivity to disturbances.

3.1.2. Dynamic simulations

To evaluate the system’s stability, it is necessary to perform dynamic simulations after a disturbance and analyze the transient behavior of voltages and frequencies. This allows for determining whether the system can return to a stable operating condition or if instability, such as voltage collapse or generator loss of synchronism, occurs.

For the “savnw” test case, dynamic simulations were performed in the PSS/E software for the machine trips at the selected buses, as per Table 1. The disturbance clearing time is assumed to be one period.

For the electrical machines included in the clusters, the original GENROU and GENSAL generator models, which are featured for capturing detailed electromagnetic transients, are used. For the external system, the complex generator models are replaced with a simple GENCLS model [33], which includes the generator in the swing equation as a simple inertia and damping system. This allows for fewer state variables (only the inertia constant and the damping coefficient are specified) per electric machine, and the excitation and governor models to be omitted. This results in lower computational burden and faster simulations.

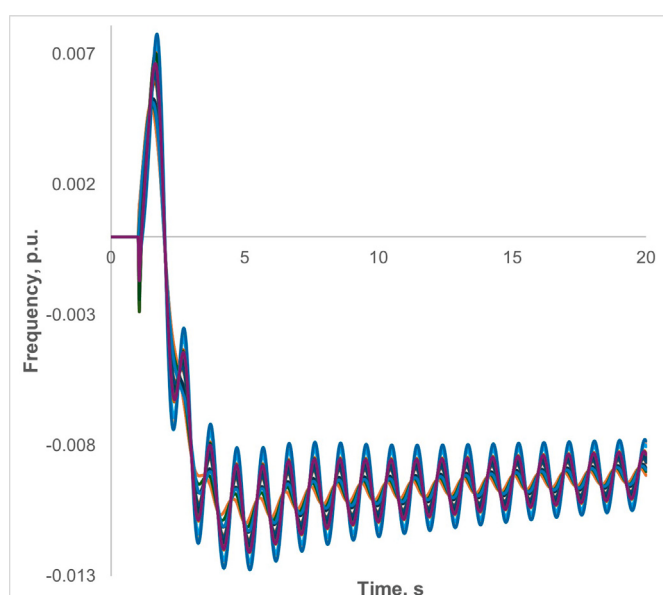


Fig. 3. Frequency trajectories after a machine trip at bus 206.

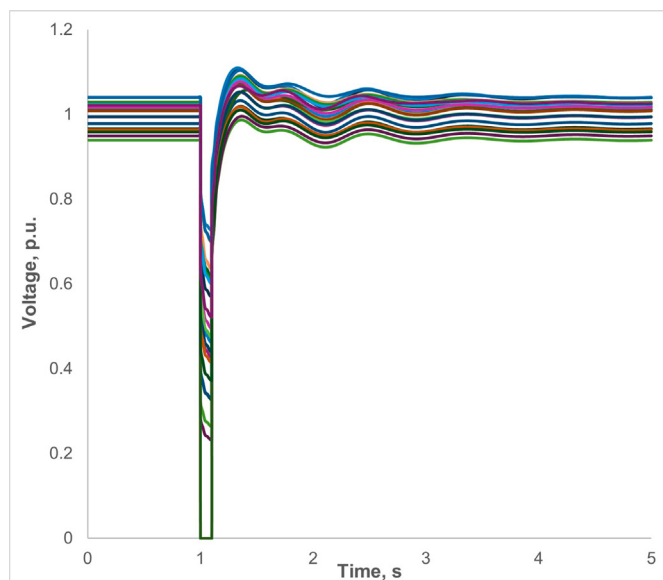


Fig. 4. Voltage trajectories after a machine trip at bus 206.

After all the experienced disturbances, the power system is able to stabilize and return to a steady state. The highest level of transient oscillations is supervised after a trip of the 800 MW generation unit at Bus 206, which is the largest machine in the system. The frequency trajectories in per-unit for this case are shown in Fig. 3. Initially, there is a sharp deviation in the frequency due to the machine disconnection, followed by oscillations that gradually diminish as the system approaches a new steady state. Although the frequency oscillations persist beyond the simulation time, their magnitude is small, less than $1 \cdot 10^{-3} \text{ p.u.}$, and the system appears to stabilize completely after around 15–20 s.

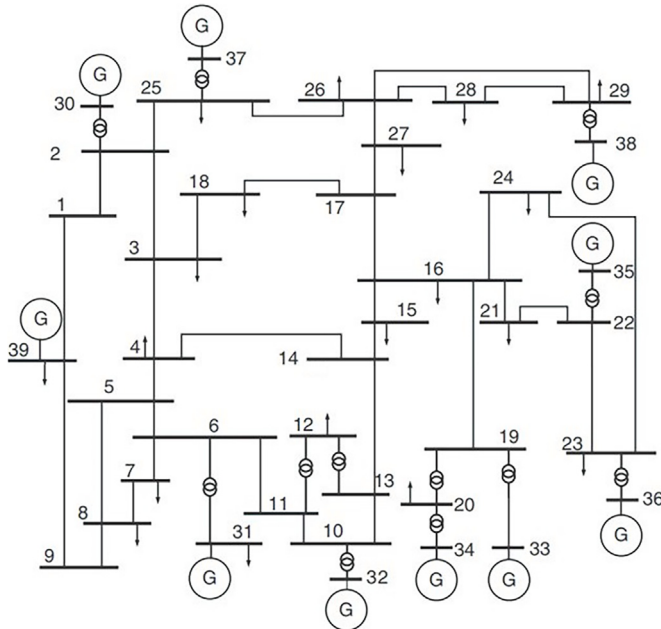
The voltage trajectories in Fig. 4 suggest that voltages at the system buses recover fast and come to their post-fault levels after clearing the fault.

An idea about the time for which a disturbance can be applied without causing the power system’s instability can be obtained from the CrCT

Table 3

Average CrCT for the clusters formed with different approaches for the “savnw” test case.

Starting bus/faulted bus	Average CrCT for electrical-distance-centered clusters		Average CrCT for clusters based on post-disturbance voltage sag	
	Seconds	Cycles	Seconds	Cycles
101	0.708452	42.50714	0.560313	33.61875
102	0.708452	42.50714	0.560313	33.61875
154	0.720357	43.22143	0.608625	36.5175
206	0.708452	42.50714	0.552441	33.14643
211	0.721000	43.26000	0.562949	33.77692
3011	0.569203	34.15217	0.646041	38.7625
3018	0.670917	40.25500	0.260834	15.6500
Average	0.686690	41.20143	0.535931	32.15584

**Fig. 5.** Single-line diagram of the IEEE 39 bus test case.

values. Calculations of CrCT were performed using the PSS/E embedded functionality for the clustered buses from [Table 1](#) and [Table 2](#). The rotor angle threshold is set to 180°. The rotor angle calculation is based on the relative to the system average rotor angle. If the system remains stable after 50 cycles (0.833333 s) of disturbance, then the CrCT calculation is terminated, assuming that more prolonged disturbances are unrealistic in transmission power systems. The CrCT value at the considered location is then taken as equal to the calculation stop time.

The average CrCT times for the bus clusters formed according to the electrical-distance-centered approach with graph theory and with the method based on the post-disturbance voltage sag are compared in [Table 3](#), where the last row shows the mean CrCT across all the clusters.

In most cases, the method based on the voltage sag estimation selects buses with smaller CrCT values. On average, the CrCT for the clusters formed with the method based on the post-disturbance voltage sag is 21.96 % smaller than that of the CrCT for the clusters built with the proposed approach. Such results could be expected because the clustering based on the post-disturbance voltage sag inherently reflects the impedance relationships between buses in the power system. Since buses closer to the fault have lower path impedance between themselves and the faulted bus, the voltage and current changes occur with faster dynamics. Therefore, the clustered buses should have smaller CrCTs, as the system requires quicker fault clearance to avoid instability.

Table 4

Results of electrical-distance-centered cluster formation using graph theory for the IEEE 39-bus system.

Starting bus	Clustered buses
14	1, 4, 5, 6, 7, 8, 9, 10, 11, 12, 13, 14, 31, 32, 39
30	5, 6, 7, 8, 10, 11, 12, 13, 30, 31, 32
33	4, 5, 6, 7, 8, 9, 10, 11, 12, 13, 31, 32, 33
35	5, 6, 7, 8, 9, 10, 11, 12, 13, 31, 32, 35
36	5, 6, 7, 8, 10, 11, 12, 13, 31, 32, 36
37	5, 6, 7, 8, 10, 11, 12, 13, 31, 32, 37
39	4, 5, 6, 7, 8, 10, 11, 12, 13, 14, 31, 32, 39

3.2. IEEE 39-bus power system

3.2.1. Cluster formation

The IEEE 39-bus system, [Fig. 5](#), consists of 10 generators, 46 branches (including transformers and overhead lines), and 19 loads and is widely used for studies related to power flow, voltage and angular stability, state estimation, and control in electrical grids [35]. This IEEE 39-bus test case includes GENROU and GENSAL synchronous generator models, IEEEET1 exciter model, IEEEG1 and IEEEG3 governor models for dynamic simulations [33].

The results of the cluster margins' determination for the IEEE 39-bus power system are shown in [Table 4](#). The cluster-forming threshold, $\xi_{\text{threshold}}$, was set to 0.03 for all the considered generation buses. Clustering using Floyd–Warshall's and Dijkstra's algorithms produced similar results, confirming the correctness of the implementation.

From [Table 4](#), it can be seen that, e.g., the cluster formed around the power plant at Bus 30 is comprised of 11 buses of the system, at Bus 35 – of 12 buses, at Bus 39 – of 13 buses. On average, a cluster contains 12.13 buses. The buses numbered from 5 to 8 and from 10 to 13 are present in all cluster-forming scenarios from [Table 4](#), which suggests their potential vulnerability to disturbances in the power system.

Next, the clusters for the IEEE 39-bus system were formed based on the voltage sag after a fault. Three-phase short circuit faults were applied at the same starting buses as per [Table 4](#). The voltage threshold for this case is assumed to be $V_{\text{lim}}^{\max} = 0.8 \text{ p.u.}$ Any buses where the voltage drops below this threshold are considered severely impacted by the disturbance and will be grouped into a cluster. The simulation results are summarized in [Table 5](#).

From [Table 5](#), it can be seen that the cluster formed around Bus 30 consists of 18 buses, around Bus 35 – of 14 buses, and around Bus 3011 – of 20 buses of the IEEE 39-bus power system. Overall, the clusters formed with the method based on the post-disturbance voltage sag are bigger than those formed according to the electrical-distance-centered approach using graph theory. An average cluster from [Table 5](#) contains 14.88 buses. The bus numbers in the clusters differ depending on the fault location, and it is difficult to distinguish particular locations that would be more prone to instability during the fault compared to the others.

Table 5

Results of cluster formation for the IEEE 39-bus system, based on the post-disturbance voltage sag.

Starting bus	Clustered buses
14	2, 3, 4, 5, 6, 7, 8, 9, 10, 11, 12, 13, 14, 15, 16, 17, 18, 19, 20, 21, 22, 23, 24, 25, 26, 27, 31, 32, 33, 35
30	1, 2, 3, 4, 5, 7, 12, 14, 15, 16, 17, 18, 25, 26, 27, 28, 30, 37
33	14, 15, 16, 17, 18, 19, 20, 21, 22, 23, 24, 27, 33, 34
35	14, 15, 16, 17, 18, 19, 20, 21, 22, 23, 24, 27, 35, 36
36	15, 16, 17, 21, 22, 23, 24, 35, 36
37	2, 3, 17, 18, 25, 26, 27, 28, 37
39	1, 2, 3, 4, 5, 6, 7, 8, 9, 10, 11, 12, 13, 14, 15, 18, 25, 31, 32, 39

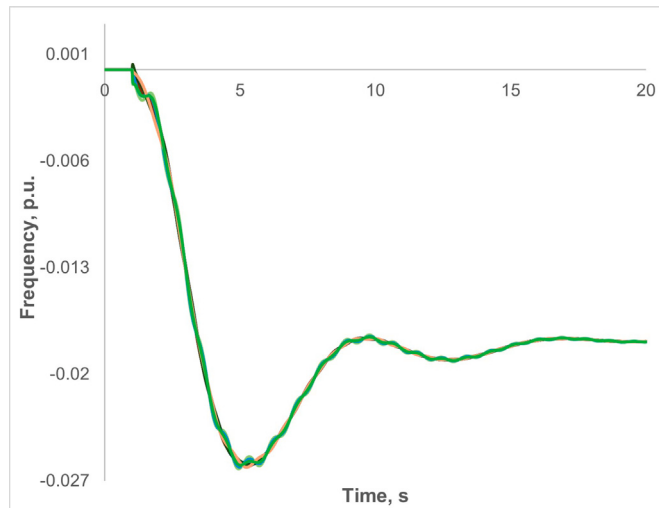


Fig. 6. Frequency trajectories after a machine trip at bus 39.

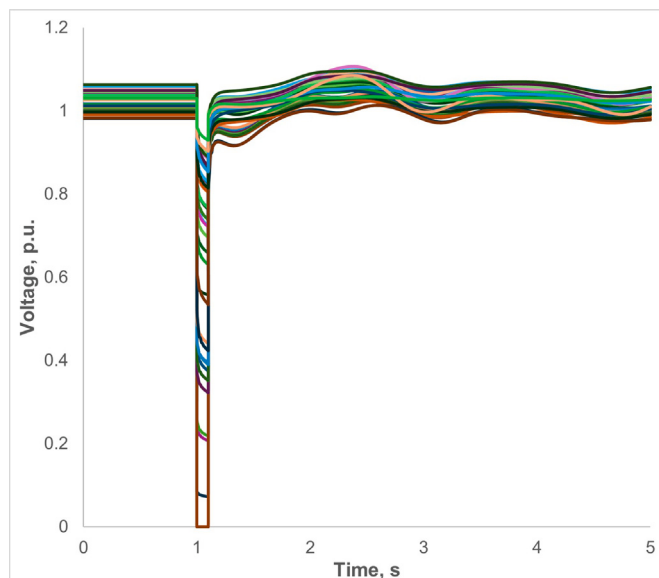


Fig. 7. Voltage trajectories after a machine trip at bus 39.

3.2.2. Dynamic simulations

A series of dynamic simulations was performed to evaluate the stability of the IEEE 39-bus system after disturbances. Tripping of generation units at the selected buses was simulated as per Table 4. The disturbance clearing time of one period is assumed. For the generators included in the clusters, the detailed GENROU and GENSAL dynamic models are used.

For the portion of the power system not included in the clusters, the detailed generator models are replaced with a simple GENCLS model with only inertia and damping values specified. In this case, the generator will respond to frequency deviations but will not have transient electrical dynamics. The governor and exciter models are omitted to further reduce the computational burden and accelerate the simulations.

The power system is able to reestablish equilibrium after all the tested disturbances. Fig. 6 shows the frequency trajectories supervised after a trip of the 1000 MW generation unit at Bus 39, which is the largest machine in the system. Initially, the frequency deviates sharply due to the unit disconnection, followed by some minor oscillations that quickly attenuate as the system returns to its steady state.

The voltage trajectories in Fig. 7 demonstrate that the bus voltages recover fast to their post-fault levels after clearing the fault.

Next, calculations of CrCT were performed for the clustered buses from Table 4 and Table 5. The rotor angle threshold is set to 180°. If the system remains stable after 50 cycles (0.833333 s) of disturbance, the CrCT calculation is terminated, assuming that longer disturbances are unlikely in transmission power systems. The CrCT value at the given location is then considered equal to the calculation stop time.

The average CrCT times for the bus clusters formed according to the proposed approach and with the method based on the post-disturbance voltage sag are compared in Table 6, where the last row specifies the average CrCT values across the clusters.

For the IEEE 39-bus system, the method based on the voltage sag estimation often creates clusters of buses with smaller CrCT values. On average, the CrCT for the clusters built with the method based on the post-disturbance voltage sag is 14.22 % smaller compared to the CrCT for the clusters created with the proposed approach. These results could be anticipated based on the same considerations as for the “savnw” test case, as elaborated in Section 3.2.

3.3. Comparison of simulations with full and reduced models

A simulation with GENCLS models used in the portion of the power system not included in the clusters is expected to run faster than a simulation using detailed generator models for the same power system. To assess this difference, dynamic simulations were run in the PSS/E software for the machine trips at the selected buses, according to the electrical-distance-centered clustering, with full and reduced dynamic models. During the simulations, it was checked that the power system with reduced dynamic models adequately captures the critical dynamics: the time-domain plots for frequency response trends and voltage deviations during and after the considered disturbances have high similarity with those obtained for the full dynamic model, and the rotor angle differences between the clustered generators are negligible.

Table 7 compares simulation times for the “savnw” and IEEE 39-bus power systems with full and reduced dynamic models, showing the results in ms. The simulations were performed on a workstation equipped with an Intel Core i7-1365U processor, 64 GB of DDR4 RAM, and a Windows 11 Pro operating system.

As can be seen, simulations with reduced dynamic models are faster than simulations with full dynamic models across all the scenarios. The average time of dynamic simulations for the “savnw” power system with reduced dynamic models is 357.426 ms, which is 14.94 % faster compared to simulations with full dynamic models, which require 410.819 ms, on average. For the IEEE 39-bus system, simulations with reduced dynamic models require, on average, 17.14 % less time to complete, compared to the simulations with full dynamic models. The difference in the computational time is more considerable for the IEEE 39-bus system with 10 generators compared to the “savnw” test case with 6 generators.

3.4. Limitations of the proposed approach

Clustering using graph theory and the concept of electrical distance incorporates a global view of the power network, considering the entire

Table 6

Average CrCT for the clusters formed with different methods for the IEEE 39-bus system.

Starting bus/faulted bus	Average CrCT for electrical-distance-centered clusters		Average CrCT for clusters based on post-disturbance voltage sag	
	Seconds	Cycles	Seconds	Cycles
14	0.352972	21.17833	0.23425	14.055
30	0.266402	15.98409	0.278032	16.68194
33	0.268654	16.11923	0.202589	12.15536
35	0.277153	16.62917	0.212262	12.73571
36	0.243637	14.61818	0.208519	12.51111
37	0.237008	14.22045	0.199306	11.95833
39	0.289487	17.36923	0.325208	19.5125
Average	0.276473	16.58838	0.237167	14.22999

Table 7

Simulation times for the power systems with full and reduced dynamic models, ms.

Fault at bus no	SAVNW system		Fault at bus no	IEEE 39-bus system	
	Full	Reduced		Full	Reduced
101	370.204	348.350	14	444.693	323.119
102	434.529	358.655	30	422.327	392.467
154	449.896	371.107	33	378.270	368.431
206	356.436	347.850	35	407.482	380.956
211	412.070	326.669	36	399.214	352.418
3011	409.988	358.470	37	436.378	327.964
3018	442.612	390.880	39	408.084	327.218
Average	410.819	357.426	Average	413.778	353.225

topology and relationships between buses, which is an obvious advantage. Another strength of the proposed solution is that the average size of the created clusters is smaller than that obtained with the standard method based on the post-disturbance voltage sag. This means that the reduced models of power systems would contain fewer dynamic parameters, enabling faster simulations and simplifying the analysis. However, the novel approach has several limitations that should be further discussed.

Firstly, the graph theory metrics are topology-dependent, meaning their value can vary depending on the power system's structure and the transmission connections' impedance. Therefore, integrating electrical distance with graph theory metrics requires a good understanding of the properties of a power system under consideration. Clustering results should be updated after each network reconfiguration. Additionally, while graph theory provides a structural view of power networks, it does not distinguish generation and load nodes, which may be a limiting factor in clustering for stability and operational efficiency.

Secondly, the computational and memory burden of the filtering by electrical distance increases proportionally to the size of the power system under study. The reason for that is mainly in the matrix inversion procedure [32], which is required to obtain an impedance matrix from an admittance matrix. The resulting impedance matrix will be proportional to the square size of its admittance matrix, and the electrical distance matrix is then derived from the impedance matrix. Different decomposition techniques, as per Section 2, can be applied to mitigate the computational and memory burden.

Also, it should be noted that the sparsity/density of the inverted matrix should not be treated as a direct indicator of the connectivity of the power system's graph. This is because the density/sparsity of the inverted matrix is influenced by the specific properties of the electrical network, such as connectivity, the arrangement of branches and buses, and the physical layout.

In summary, to ensure the accuracy and representativeness of the results, the selection of parts and elements for simulations should be made carefully based on the TSO's expertise and knowledge of the power system's model. This would help to ensure that the formed subsets of buses adequately capture the dynamic interactions and feedback effects within the power system.

4. Conclusions

With the increasing risk of operational disruptions caused by terrorist and military attacks on critical energy infrastructure and power-generating plants, the need for quick operating solutions to avoid wide-area blackouts has become paramount. Besides that, variations in wind and solar power generation can cause disruptions in bulk power systems, especially as their penetration increases. However, the simulation of bulk power systems in dynamics and even in statics is associated with the challenges of extra complexity, the long time needed for obtaining the solution, and limitations imposed by the computational capacity of the software tools. To overcome these limitations while ensuring the accuracy of the solution, detailed simulations can be performed only for a part of the bulk power system, which is expected to be most influenced by a disruption. The portion of the bulk system that is not explicitly modeled can be replaced by an equivalent with similar behavior, or full dynamic generator models in that portion of the system can be replaced with simpler models with fewer state variables.

This study proposes a clustering approach based on electrical distance and graph theory. Compared with traditional clustering methods, the proposed solution captures both the topological and electrical connectivity of power systems, ensuring more accurate identification of vulnerable areas. It can be used by transmission system operators to perform studies on the system's stability, facilitating quick operational decisions after disruptions. Additionally, this approach can be adapted by grid planners for resiliency studies and the integration of renewable energy sources into bulk power systems. By clustering the system based on electrical distance and graph theory, regions where RES integration poses challenges, such as variability in power output and demand response, can be analyzed more efficiently.

Although the electrical-distance-centered clustering using graph theory can be advantageous given its interdependence with the network's power propagation and electrical connectedness, its adoption would require the user's sound understanding of graph theory and the specifics of a power system under study.

Future work will focus on cluster formation to improve resiliency, helping power systems withstand and adapt to unexpected disruptions while minimizing downtime and service interruptions.

CRediT authorship contribution statement

Illia Diahovchenko: Writing – review & editing, Validation, Investigation, Visualization, Methodology, Conceptualization, Writing – original draft, Software, Data curation. **Andrew Keane:** Project administration, Writing – review & editing, Formal analysis, Funding acquisition.

Declaration of competing interest

The authors declare that they have no known competing financial interests or personal relationships that could have appeared to influence the work reported in this paper.

Acknowledgment

The research conducted in this publication was funded by **Science Foundation Ireland** and co-funding partners under grant number **21/SPP/3756** through the **NexSys Strategic Partnership Programme**.

Data availability

Data will be made available upon request.

References

- [1] J. Khazaei, Cyberattacks with limited network information leading to transmission line overflow in cyber-physical power systems, *Sustain. Energy Grids Netw.* 27 (2021) 100505.
- [2] L. Tichy, Energy infrastructure as a target of terrorist attacks from the islamic state in Iraq and Syria, *Int. J. Crit. Infrastruct. Protect.* 25 (2019) 1–13.
- [3] J.L. Sowers, E. Weinthal, N. Zawahri, Targeting environmental infrastructures, international law, and civilians in the new middle eastern wars, *Secur. Dialogue* 48 (5) (2017) 410–430.
- [4] A. Malenko, Ukraine races to fix and shield its power plants after Russian onslaught, April 2024. [Online]. Available: <https://www.reuters.com/world/europe/ukraine-races-fix-shield-its-power-plants-after-russian-onslaught-2024-04-09/>.
- [5] International Energy Agency (IEA), Ukraine's energy security and the coming winter, Paris, 2024. [Online]. Available: <https://www.iea.org/reports/ukraines-energy-security-and-the-coming-winter>.
- [6] UN Human Rights Monitoring Mission in Ukraine, Attacks on ukraine's energy infrastructure: harm to the civilian population, Kyiv, September 2024, [Online]. Available: <https://ukraine.un.org/en/278992-attacks-ukraine%E2%80%99s-energy-infrastructure-harm-civilian-population>.
- [7] E. Ingram, IEA reports Russia's attacks on ukraine's energy sector have escalated as winter sets in, January 2024, [Online]. Available: <https://www.hydroreview.com/business-finance/business/iea-reports-russias-attacks-on-ukraines-energy-sector-have-escalated-as-winter-sets-in/>.
- [8] I. Koshiw, Russian offensive campaign assessment, april 8, 2024, April 2024, [Online]. Available: <https://www.ft.com/content/18882abd-6277-4aae-bc43-f3e5fa786445>.
- [9] DiXi Group, Russian war against Ukraine: energy dimension | dixi group alert – weekly review, April 2024, [Online]. Available: <https://dixigroup.org/en/analytic/russian-war-against-ukraine-energy-dimension-dixi-group-alert-weekly-review-46/>.
- [10] ENTSO-E, Ukrainian transmission system operator NPC Ukrrenergo, joins ENTSO-E as new member, 2023, [Online]. Available: <https://www.entsoe.eu/news/2023/12/14/ukrainian-transmission-system-operator-npc-ukrrenergo-joins-entso-e-as-new-member/>.
- [11] Kimdime, Map of European transmission system operators organizations (regional groups), 2023. [Online]. Available: <https://upload.wikimedia.org/wikipedia/commons/6/6d/ElectricityUCTE.svg>.
- [12] Energy Institute, Statistical Review of World Energy, 73rd ed., Energy Institute, 2024. [Online]. Available: <https://www.energyinst.org/statistical-review>.
- [13] I. Diahovchenko, Z. Viacheslav, Optimal composition of alternative energy sources to minimize power losses and maximize profits in distribution power network, in: 2020 IEEE 7th International Conference on Energy Smart Systems (ESS), IEEE, 2020, pp. 247–252.
- [14] I.M. Diahovchenko, G. Kandaperumal, A.K. Srivastava, Enabling resiliency using microgrids with dynamic boundaries, *Electr. Power Syst. Res.* 221 (2023) 109460.
- [15] I.M. Diahovchenko, G. Kandaperumal, A.K. Srivastava, Z.I. Maslova, S.M. Lebedka, Resiliency-driven strategies for power distribution system development, *Electr. Power Syst. Res.* 197 (2021) 107327.
- [16] I. Diahovchenko, A. Keane, Boundary estimation of vulnerable areas in bulk power systems using electrical distance, in: 2024 IEEE PES Innovative Smart Grid Technologies Europe (ISGT EUROPE), 2024, pp. 1–5.
- [17] P. Lagonotte, J.C. Sabonnadiere, J.-Y. Leost, J.-P. Paul, Structural analysis of the electrical system: application to secondary voltage control in France, *IEEE Trans. Power Syst.* 4 (2) (1989) 479–486.
- [18] K. Visakha, D. Thukaram, L. Jenkins, Transmission charges of power contracts based on relative electrical distances in open access, *Electr. Power Syst. Res.* 70 (2) (2004) 153–161.
- [19] S. Blumsack, P. Hines, M. Patel, C. Barrows, E.C. Sanchez, Defining power network zones from measures of electrical distance, in: 2009 IEEE Power and Energy Society General Meeting, PES '09, 2009.
- [20] E. Cotilla-Sánchez, P.D.H. Hines, C. Barrows, S. Blumsack, M. Patel, Multi-attribute partitioning of power networks based on electrical distance, *IEEE Trans. Power Syst.* 28 (4) (2013) 4979–4987.
- [21] S. Poudel, Z. Ni, W. Sun, Electrical distance approach for searching vulnerable branches during contingencies, *IEEE Trans. Smart Grid* 9 (4) (2018) 3373–3382.
- [22] X. Mao, W. Zhu, L. Wu, B. Zhou, Comparative study on methods for computing electrical distance, *Int. J. Electr. Power Energy Syst.* 130 (2021) 106923.
- [23] M. Baranwal, S. Salapaka, Clustering and supervisory voltage control in power systems, *Int. J. Electr. Power Energy Syst.* 109 (2019) 641–651.
- [24] S.F. Mahdavizadeh, M.R. Aghamohammadi, S. Ranjbar, Frequency stability-based controlled islanding scheme based on clustering algorithm and electrical distance using real-time dynamic criteria from wams data, *Sustain. Energy Grids Netw.* 30 (2022) 100560.
- [25] P. Cuffe, A. Keane, Visualizing the electrical structure of power systems, *IEEE Syst. J.*, 11 (3) (2017).
- [26] P. Hines, S. Blumsack, E.C. Sanchez, C. Barrows, The topological and electrical structure of power grids, in: Proceedings of the Annual Hawaii International Conference on System Sciences, 2010.
- [27] Y. Koç, M. Warnier, P.V. Mieghem, R.E. Kooij, F.M.T. Brazier, The impact of the topology on cascading failures in a power grid model, *Phys. A Stat. Mech. Appl.* 402 (2014) 169–179.
- [28] D. Falabretti, G. Sabbatini, A new clustering method for the optimization of distribution networks layout considering energy efficiency and continuity of service, *Sustain. Energy Grids Netw.* 30 (2022) 100654.
- [29] M. Kazim, H. Pirim, S. Shi, D. Wu, Multilayer analysis of energy networks, *Sustain. Energy Grids Netw.* 39 (2024) 101407.
- [30] M.A. Djojo, K. Karyono, Computational load analysis of Dijkstra, A*, and Floyd-Warshall algorithms in mesh network, in: 2013 International Conference on Robotics, Biomimetics, Intelligent Computational Systems, IEEE, 2013, pp. 104–108.
- [31] R.T. Senthil, Blockwise inversion and algorithms for inverting large partitioned matrices, 2023, arXiv preprint arXiv:2305.11103.
- [32] T.H. Cormen, C.E. Leiserson, R.L. Rivest, C. Stein, *Introduction to Algorithms*, MIT Press, 2022.
- [33] Siemens Power Technologies International, Program Application Guide PSS®E 35.6.1, vol. 2, Siemens Industry, Inc., 2023.
- [34] A. Papaemmanouil, G. Andersson, On the reduction of large power system models for power market simulations, in: 17th Power Systems Computation Conference (PSCC), Citeseer, 2011, pp. 1308–1313.
- [35] C. Canizares, T. Fernandes, E. Geraldi Jr, L. Gerin-Lajoie, M. Gibbard, I. Hiskens, J. Kersulis, R. Kuiava, L. Lima, F. Marco, et al, Benchmark systems for small signal stability analysis and control, no. PES-TR, 2015, <http://resourcecenter.ieee-pes.org/pes/product/technical-reports/PESTR18>.